Farshid Bagheri[1]
Laboratory for Alternative Energy Conversion (LAEC),
School of Mechatronic Systems Engineering,
Simon Fraser University,
Surrey, BC V3T 0A3, Canada
e-mail: fbagheri@sfu.ca

M. Ali Fayazbakhsh
Laboratory for Alternative Energy Conversion (LAEC),
School of Mechatronic Systems Engineering,
Simon Fraser University,
Surrey, BC V3T 0A3, Canada

Majid Bahrami[1]
Laboratory for Alternative Energy Conversion (LAEC),
School of Mechatronic Systems Engineering,
Simon Fraser University,
Surrey, BC V3T 0A3, Canada
e-mail: mbahrami@sfu.ca

Investigation of Optimum Refrigerant Charge and Fans' Speed for a Vehicle Air Conditioning System

In this study, the performance evaluation and optimization of a recently developed battery-powered vehicle air conditioning (BPVAC) system is investigated. A mathematical model is developed to simulate the thermodynamic and heat transfer characteristics of the BPVAC system and calculate the coefficient of performance (COP). Utilizing environmental chambers and a number of measuring equipment, an experimental setup is built to validate the model accuracy and to conduct performance optimization by changing the charge of refrigerant in the system. The model is validated and employed for performance simulation and optimization in a wide range of speed for the evaporator and condenser fans. The modeling results verify that for any operating condition an optimum performance can be achieved by adjusting the speed of condenser and evaporator fans. The optimum refrigerant charge is obtained, and a potential improvement of 10.5% is calculated for the performance of system under ANSI/AHRI 210/240-2008 specifications.
[DOI: 10.1115/1.4034852]

Keywords: performance, optimization, air conditioning, vehicle, battery-powered

1 Introduction

Legislation of anti-idle rules as well as mass production of hybrid and electric vehicles during the past years have been promising signs of green and sustainable energy development in transportation industry. Air conditioning and refrigeration (A/C–R) as one of the major energy consuming components in the transportation industry plays a key role in green and sustainable energy development. The anti-idle rules and electric vehicle development have brought to wide utilization of battery-powered air conditioning systems. Idling vehicle engines, which is defined as running the engine to power the auxiliaries while the vehicle is not moving, consumes a tremendous amount of energy leading to large quantities of greenhouse gas emissions. Only in the U.S., idling consumes about 6×10^9 gal of oil and causes emissions of more than 130 ton of particulate matter, 12×10^6 ton of CO_2, 35,000 ton of NO_x, and 36,000 ton of CO each year [1,2]. In response to the increasing awareness of the adverse effects of idling engines on human health and environment, many cities around the world have instituted idling restrictions and bans especially for long-haul trucks. The idling limitation has caused a major difficulty for truck drivers and created a great demand for the battery-powered air conditioning systems [1,3]. MacDonald et al. [4] generally assessed alternative anti-idle air conditioning systems that can respond to this demand. They concluded that the battery-powered vehicle air conditioning (BPVAC) system is one of the promising alternatives toward eliminating the engine idling. Due to impact of BPVAC systems on the global fuel consumption and environment, a performance evaluation and optimization study on these systems is required.

Although there are numerous studies in the literature with focus on air conditioning (A/C) system in different applications, the number of studies relevant to general category of vehicle air conditioning (VAC) systems is restricted [5–14]. In addition, due to harsher working environment caused by sun exposure, lack of appropriate insulation of conditioned spaces, movement of the vehicle, and frequent door opening for loading or unloading purposes, the coefficient of performance (COP) is relatively low in VAC systems. However, while the performance evaluation and optimization of the stationary A/C systems have been included in several studies, the literature lacks comprehensive studies on the performance optimization of the VAC systems. Al-Rashed [13] studied the effects of evaporator temperature on the COP of a stationary vapor compression refrigeration system and obtained an optimal COP by changing this temperature. Green et al. [12] introduced a performance function that encompassed food quality, energy efficiency, and system reliability, to enable performance assessment and optimization of a supermarket refrigeration system. They studied the effects of thermostatic set point temperature as the control parameter to optimize the defined performance function. Sahin and Kodal [14] presented a finite-time thermoeconomic performance model for a two-stage refrigerator and determined the optimal operation and design parameters of the refrigerator based on the thermoeconomic criterion. They mainly focused on the effects of investment and energy costs in designing a high-efficiency cascade refrigerator and demonstrated that the economical parameter had a great influence on the optimal operating and design parameters.

A majority of the studies in the field of VAC systems is related to assessment of refrigerant type effects on the characteristic and the performance [11,15–18]. A variety of other important parameters including refrigerant charge, compressor speed, and ambient temperature have also been considered through the VAC system studies. Ratts and Brown [19] experimentally analyzed the COP of a passenger car A/C system focusing on relationships between the COP, the compressor revolution, and the vehicle speed. Their analysis showed that the performance of the system degraded by increasing the vehicle speed. Wang et al. [20] experimentally showed that the COP of a VAC system decreased by increment of the refrigerant charge, condensing temperature, and compressor speed, and increased by increment of the evaporator air inlet temperature. They reported the value of COP in the range of 1.1–2.5 for a variety of operating condition. Macagnan et al. [21]

[1]Corresponding author.

Contributed by the Heat Transfer Division of ASME for publication in the Journal of Thermal Science and Engineering Applications. Manuscript received January 7, 2016; final manuscript received August 10, 2016; published online November 8, 2016. Assoc. Editor: Wei Li.

experimentally investigated into the effects of refrigerant charge and compressor speed on the cooling power and performance of a typical VAC and showed that although the refrigerant charge did not sensibly affect the VAC system characteristics, the compressor speed caused a variation of the system COP in a range of 1–1.8.

Alkan and Hosoz [22] experimentally compared a variable capacity compressor (VCC) and a fixed capacity compressor (FCC) for a VAC system in different engine rotational speeds as well as evaporator and condenser air stream characteristics. It was shown that although the COP of VCC system during low-engine rpm operations is slightly poorer, it surpasses the COP of FCC system at higher rpms. Moreover, the COP of FCC system decreases persistently by the compressor speed increment. Jabardo et al. [23] studied the effects of compressor speed and the evaporator and condenser inlet air temperatures on the performance of a VAC by developing a steady-state thermodynamic simulation model. The transient behavior of a VAC system was studied by Tian and Li [24] using a quasi-steady-state model. Also, the effects of refrigerant charge and condenser size on the performance of a typical VAC were studied by Lee and Yoo [10] based on a mathematical model.

The comprehensive literature review indicates that the performance evaluation of BPVAC has not been studied in-depth, and the pertinent literature lacks the following:

- performance behavior of BPVAC systems under realistic operating conditions.
- performance optimization of an existing BPVAC system by adjusting the fans' speeds and refrigerant charge. This concept will be expandable to any existing air conditioning and refrigeration system and applicable with no cost or changes in the system elements or configuration.

The present study aims to develop a mathematical model as well as an experimental setup for investigating the performance characteristics of a currently used BPVAC unit in trucks for anti-idling purposes. The study includes a comprehensive performance evaluation of the unit toward finding the optimum performance for a variety of refrigerant charge as well as condenser and evaporator fans' speeds, which are practical with no cost or changes on the system configuration. The results of this study are expandable to any A/C system and can be employed in future for developing an intelligent control module to adjust the fans' speeds for optimal operation achievement under any ambient condition.

2 Mathematical Model

In this section, a mathematical model is developed for evaluating the performance of BPVAC system and to simulate thermodynamic parameters under various working conditions. The major output parameter from the modeling of any A/C system is the coefficient of performance (COP = cooling power/input power). In addition to the COP, other parameters of an A/C system, including cooling power, input power, and refrigerant mass flow rate, are obtained from the modeling results.

2.1 Compressor Model. Based on volumetric, electrical, and mechanical efficiencies of a compressor, its thermodynamic model can be developed [8,25]. It was shown that this approach had a good agreement with experimental data [26]. As such, the refrigerant mass flow rate and power consumption by the compressor can be obtained using Eqs. (1) and (2) provided in Table 1. These equations yield a maximum of 1.8% discrepancy when compared to the manufacturer's data. Based on these equations, with known inlet conditions, the state point of refrigerant gas at the compressor discharge can be determined.

2.2 Condenser and Evaporator Models. Energy balance correlations between the refrigerant and air flows in condenser and evaporators are used to model heat transfer in these components. In the present study, an $\varepsilon - \mathrm{NTU}$ model is employed to derive the mathematical model for the condenser and evaporator [27]. In this approach, the effectiveness ε is defined as the ratio of the actual heat transfer to the maximum possible heat transfer, which Eq. (3), see Table 1. The maximum possible heat transfer is defined in Eq. (4). The actual heat transfer between the air stream and the refrigerant flow can be calculated using Eq. (5). To use this equation, ε is required to be found from Eqs. (6) and (7). Furthermore, the convective heat transfer coefficients are calculated using Eqs. (8) and (9), respectively, for one-phase and two-phase regimes [27–30].

For the selected BPVAC system, the condenser and evaporator specifications are obtained from the manufacturer's data and in-lab measurements. In addition to the heat transfer model for the condenser and evaporator, map-based correlations are employed to obtain the fans' electric power consumption using manufacturer's datasheets [31], see Eq. (10) in Table 1.

2.3 Thermostatic Expansion Valve (TEV) Model. Following Ref. [32], an isenthalpic model is selected for thermodynamic simulation of the thermostatic expansion valve in the present study. In this model, as a result of adiabatic assumption, the inlet and outlet refrigerant enthalpies are considered the same, see Eq. (11).

2.4 Numerical Solver. Developing the mathematical model for BPVAC system, including Table 1 correlations and the condenser and evaporator overall heat transfer relationships as well as thermodynamic properties' correlations of HFC-134a (the most widely used refrigerant in transportation industry), leads to a set of 20 coupled nonlinear equations that has to be solved simultaneously. The BPVAC system unknown parameters $(x_1 - x_{20})$, which are calculated using the mathematical model, are listed in Table 2.

The set of coupled and nonlinear equations are arranged in the form of Eq. (12). Due to nonlinearity and coupling of these equations, a numerical method is required for the solution. As such, an iterative numerical solver is developed based on Newton–Raphson method to solve the set of complex equations [33]. During the iterative numerical solution, starting from an initial approximation the unknowns are calculated at any iteration (n) and then used for the next iteration $(n+1)$ as represented in Eq. (13). The iterative procedure continues until the maximum relative residual of the unknown parameters is less than 10^{-3}

$$\begin{cases} g_1(x_1 = \text{cooling power}, x_2 = W_{\text{comp}}, \ldots, x_{20} = h_{\text{TEV,in}}) = 0 \\ g_2(x_1 = \text{cooling power}, x_2 = W_{\text{comp}}, \ldots, x_{20} = h_{\text{TEV,in}}) = 0 \\ \vdots \\ g_{20}(x_1 = \text{cooling power}, x_2 = W_{\text{comp}}, \ldots, x_{20} = h_{\text{TEV,in}}) = 0 \end{cases} \tag{12}$$

$$\begin{bmatrix} x_1^{n+1} \\ \vdots \\ x_{20}^{n+1} \end{bmatrix} = \begin{bmatrix} x_1^{n} \\ \vdots \\ x_{20}^{n} \end{bmatrix} - \begin{bmatrix} \frac{\partial g_1}{\partial x_1} \cdots \frac{\partial g_1}{\partial x_{20}} \\ \vdots \\ \frac{\partial g_{20}}{\partial x_1} \cdots \frac{\partial g_{20}}{\partial x_{20}} \end{bmatrix}_{x_i^n}^{-1} \times \begin{bmatrix} g_1(x_i^n) \\ \vdots \\ g_{20}(x_i^n) \end{bmatrix} \tag{13}$$

3 Experimental Setup

A test-bed is designed and built to study the effect of refrigerant charge on the performance of a BPVAC system. The experimental results are also employed for model verification purpose. The test-bed is equipped with two separate environmental chambers to provide any desired temperature and humidity conditions for the

Table 1 Mathematical model correlations

Compressor submodel

$$\dot{m}_{\text{ref,comp}} = NV\rho_{\text{ref,comp,in}}\eta_v \tag{1}$$

$$W_{\text{comp}} = \frac{\dot{m}_{\text{ref,comp}}(h_{\text{ref,comp,out}} - h_{\text{ref,comp,in}})}{\eta_E\eta_M} \tag{2}$$

Condenser and evaporator submodel

$$\varepsilon = \frac{\dot{Q}}{\dot{Q}_{\max}} \tag{3}$$

$$\dot{Q}_{\max} = C_{\min}(T_{\text{hot,in}} - T_{\text{cold,in}}) \tag{4}$$

$$\dot{Q} = \varepsilon C_{\min}(T_{\text{hot,in}} - T_{\text{cold,in}}) \tag{5}$$

$$\varepsilon = \frac{1 - \exp[-\text{NTU}(1 - C^*)]}{1 - C^*\exp[-\text{NTU}(1 - C^*)]} \tag{6}$$

$$C^* = \frac{C_{\min}}{C_{\max}}, \qquad \text{NTU} = \frac{\text{UA}}{C_{\min}} \tag{7}$$

$$\text{Nu}_{1-\text{ph}} = 0.023\text{Re}^{0.8}\text{Pr}^{0.4} \tag{8}$$

$$\text{Nu}_{2-\text{ph}} = 0.023\text{Re}^{0.8}\text{Pr}^{0.4}\left[(1-\gamma)^{0.8} + \frac{3.8\gamma^{0.76}(1-\gamma)^{0.04}}{\left(\frac{P}{P_{\text{cr}}}\right)^{0.38}}\right] \tag{9}$$

$$W_f = W_{f,\text{nom}}\left(c_0 + c_1\left(\frac{\dot{m}_a}{\dot{m}_{a,\text{nom}}}\right) + c_2\left(\frac{\dot{m}_a}{\dot{m}_{a,\text{nom}}}\right)^2 + c_3\left(\frac{\dot{m}_a}{\dot{m}_{a,\text{nom}}}\right)^3\right) \tag{10}$$

Expansion valve submodel

$$h_{\text{TEV,in}} = h_{\text{TEV,out}} \tag{11}$$

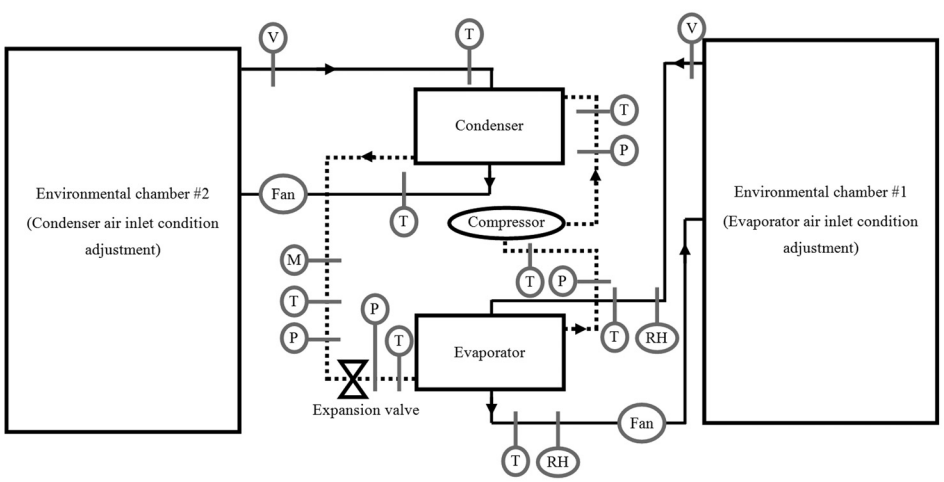

Fig. 1 Experimental setup schematic (solid lines = air flow, dashed lines = refrigerant flow, *T* = temperature sensor, *P* = pressure sensor, *M* = mass flow meter, *V* = velocity meter, and RH = relative humidity sensor)

Table 2 Output parameters of the mathematical model

Cooling power	W_{comp}	$W_{f,cond}$	$W_{f,evap}$	Heat rejection
COP	NTU_{evap}	NTU_{cond}	ε_{evap}	ε_{cond}
T_c	$h_{evap,in}$	$\dot{m}_{ref}$	T_e	h_g at T_e
$h_{comp,in}$	$h_{comp,out}$	h_g at T_c	h_f at T_c	$h_{TEV,in}$

evaporator and condenser of the BPVAC system. In addition, the test-bed consists of a BPVAC system with duct connections to the environmental chambers. The BPVAC system consists of a constant speed scroll compressor, a variable speed axial fan for condenser, a variable speed centrifugal fan for evaporator, two finned-tube coils as evaporator and condenser, a thermostatic expansion valve (TEV), a manual temperature and evaporator air speed controller, and a power control unit. Same as the most air conditioning and refrigeration systems in the transportation industry, the BPVAC is charged with HFC-134a. A schematic of the test-bed is presented in Fig. 1. A number of temperature, pressure, and relative humidity sensors as well as velocity and mass flow meters are employed in the test-bed to obtain the experimental data.

Figure 2 shows the built test-bed. The condenser-side air duct is detached for this photo to have a better vision. The employed BPVAC system is powered by DC power supplies to simulate a package of two 12 V batteries, which are directly charged by the engine alternator of vehicle in actual condition. At four spots on the evaporator and condenser air streams, T-type thermocouples with ±0.1 °C accuracy are installed. Furthermore, two wind sensors with ±0.15 m/s accuracy, refrigerant mass flow meter with 0.5% accuracy, other T-type thermocouples, and pressure transducers with 0.25% accuracy are installed at different spots of the BPVAC unit to measure the required parameters from air and refrigerant sides. The power draw by the system components is also measured directly by the DC power supplies. All the input data from thermocouples, pressure transducers, refrigerant flow meter, air velocity meters, and power supplies are collected by an

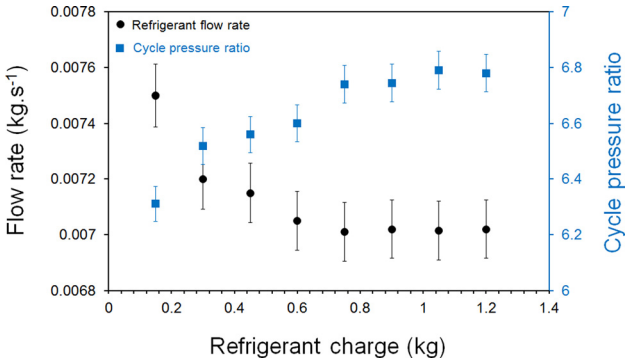

Fig. 3 Refrigerant mass flow rate and cycle pressure ratio versus refrigerant charge—experimental data

NI instrument data acquisition system (DAQ) and sent to a computer with a frequency of 60 Hz. The acquired data are then written on text files by a LABVIEW program. It should be mentioned that the maximum uncertainty for total electric power and COP measurements are ±1 W and ±0.02, respectively.

4 Results and Discussion

The main goal of this study, as a proof-of-concept demonstration for no-cost optimization of COP, is to obtain the optimum point of operation for an available BPVAC system without replacing any component of it. The only adjustable variables of such system are (1) the amount of refrigerant charge in the system and (2) the capacity of the all the controllable components. The employed system for this study is a BPVAC system described in Sec. 3 that is equipped with variable speed fans on both the evaporator and condenser sides. Accordingly, the amount of refrigerant charge, evaporator fan speed, and condenser fan speed are varied in a wide range, while the other parameters of the system are kept constant. As such, the performance behavior of the system is investigated to obtain an optimum point of operation. To keep the operational conditions constant among all of the experiments and

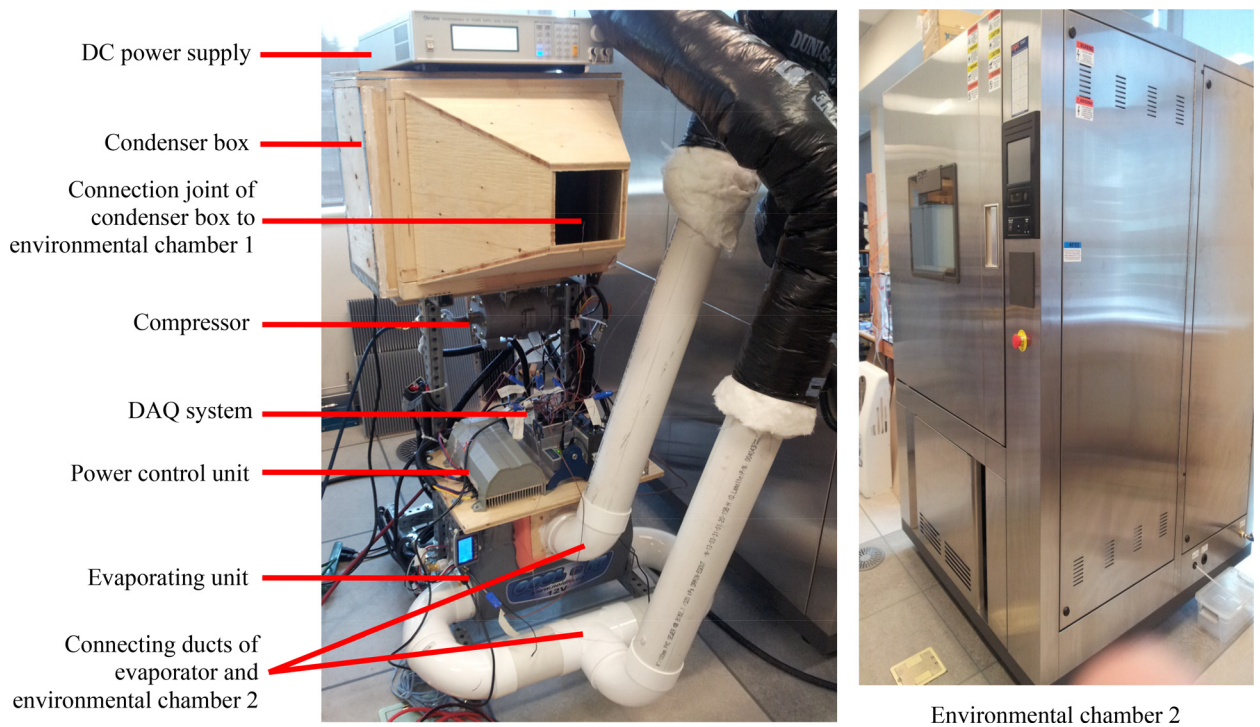

Fig. 2 Experimental setup

simulations, the standard performance requirements of ANSI/AHRI 210/240-2008 are considered in this study. However, the simulations and measurements are performed for other operational conditions, and same trends and behavioral characteristics are observed. Therefore, in this paper, only the results of tests and simulations based on ANSI/AHRI 210/240-2008 requirements are presented that are expandable to other operating conditions.

4.1 Optimum Performance by Refrigerant Charge Variation—Experimental Study. A few studies in the literature provided the behavior of COP versus refrigerant charge of A/C systems. Even though in Refs. [34] and [35] it was shown that the COP is affected by changing the refrigerant charge, Macagnan et al. [21] claimed that this effect is not sensible. Therefore, the effect of refrigerant charge on the behavior of the BPVAC system is experimentally investigated in this paper by changing the charge of HFC-134a in a wide range of 0.2–1.2 kg. Figure 3 shows the variation of refrigerant mass flow rate and cycle pressure ratio, which is defined as the ratio of condensing pressure to evaporating pressure, versus refrigerant charge. To study only the effects of refrigerant charge as a key parameter of the system, all the tests of this section are performed for the same evaporator and condenser air inlet temperatures ($T_{a,\text{evap,in}}$, $T_{a,\text{cond,in}}$) of 26.7 and 35 °C, respectively, based on ANSI/AHRI 210/240-2008. From Fig. 3, one can conclude that increasing the refrigerant charge from a small quantity (0.2 kg) first increases the cycle pressure ratio and correspondingly decreases the refrigerant mass flow rate; however, the rate of changes becomes less sensible after a specific charge (~0.75 kg). As expected, enhancement of the cycle pressure ratio by increase of the refrigerant charge has reduced the refrigerant flow rate (see Fig. 3).

Figure 4 represents the behavior of cooling power and power consumption (electrical) of the system versus refrigerant charge. The power consumption is directly measured using a digital clamp meter. In addition, the cooling power is calculated based on measured air flow rate and obtained air enthalpy at the evaporator entry and exit. The enthalpy is obtained using psychrometric data based on the dry bulb temperature and relative humidity measured during the experiments.

This figure indicates that by increasing the refrigerant charge, the cooling power first increases significantly and then slightly drops which leaves an area of maximum value around the charges of 0.6–0.75 kg. For the small charges, lack of enough refrigerant liquid to evaporate in the evaporator and provide the cooling effect is the main reason of significantly lower cooling capacity. A slight drop in the cooling power of the system after charge of 0.75 kg is due to slight increase of the evaporating temperature in the evaporator caused by a higher evaporating pressure. In fact, the increase of evaporating temperature reduces the temperature gradient between the refrigerant and air flows that lowers the cooling power of the system.

Figure 4 also shows that the system power consumption increases continuously by increasing the refrigerant charge. The power consumption increment is mainly because of the cycle pressure ratio increment that imposes higher torque on the compressor shaft.

The variation in the COP of system is also obtained from power consumption and cooling power and plotted in Fig. 5. Based on the described behavior of cooling power and power consumption of the system, the behavior of COP can be explained. Due to significant increase of the cooling power by increasing the refrigerant charge at smaller charges, the COP of the system increases remarkably. However, increasing the refrigerant charge beyond specific amount causes a reverse behavior of COP. The COP decrement after a specific charge is due to power consumption increment, while the cooling power is decreasing slightly. Thus, the system COP shows an increment–decrement behavior versus refrigerant charge that leaves a range of maximum values.

Based on the obtained results, for the BPVAC system in this study, the most appropriate refrigerant charge to achieve the maximum COP is determined as 0.75 kg. The maximum COP of the system working at nominal fans' speed and under ANSI/AHRI 210/240-2008 condition is obtained as 1.35. In Sec. 4.3, the effect of fans' speed on the COP will be investigated.

4.2 Model Verification and Performance Evaluation for Different Ambient Conditions. The developed mathematical model is first verified using the experimental data and then employed for parametric study on the effect of fans' speeds on the performance behavior of the system. In Fig. 6, four major outputs of the model simulations including refrigerant flow rate, power consumption, cooling power, and COP of the system are compared with experimental results. The simulations and experiments are performed under a wide range of operating condition to assure comprehensive accuracy verification. The results show a good agreement between simulation and experimental results. The maximum relative difference between the simulation outputs and the measured values is 10.6% emerging from cooling load results. For the rest of presented parameters, the maximum relative discrepancy between the modeled and the measured values is less than 10%.

Based on the presented results in Fig. 6, one can conclude that by increasing air temperature entering the condenser ($T_{a,\text{cond,in}}$) for any constant air temperature entering the evaporator ($T_{a,\text{evap,in}}$), the refrigerant mass flow rate increases. In addition, due to the refrigerant mass flow increase as well as the pressure ratio changes in the cycle, the total power consumption enhances by increasing $T_{a,\text{cond,in}}$. Furthermore, by increasing $T_{a,\text{cond,in}}$ for any constant $T_{a,\text{evap,in}}$, the cooling capacity of the system

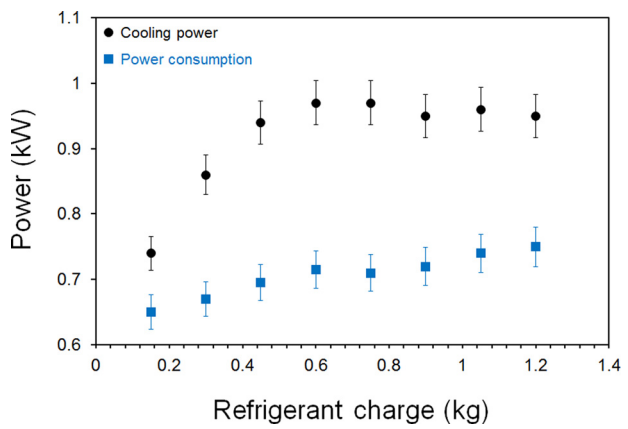

Fig. 4 Cooling power and total power consumption versus refrigerant charge—experimental data

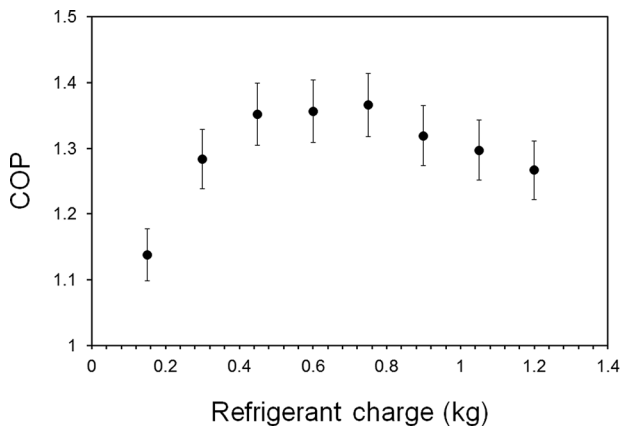

Fig. 5 COP versus refrigerant charge—experimental data

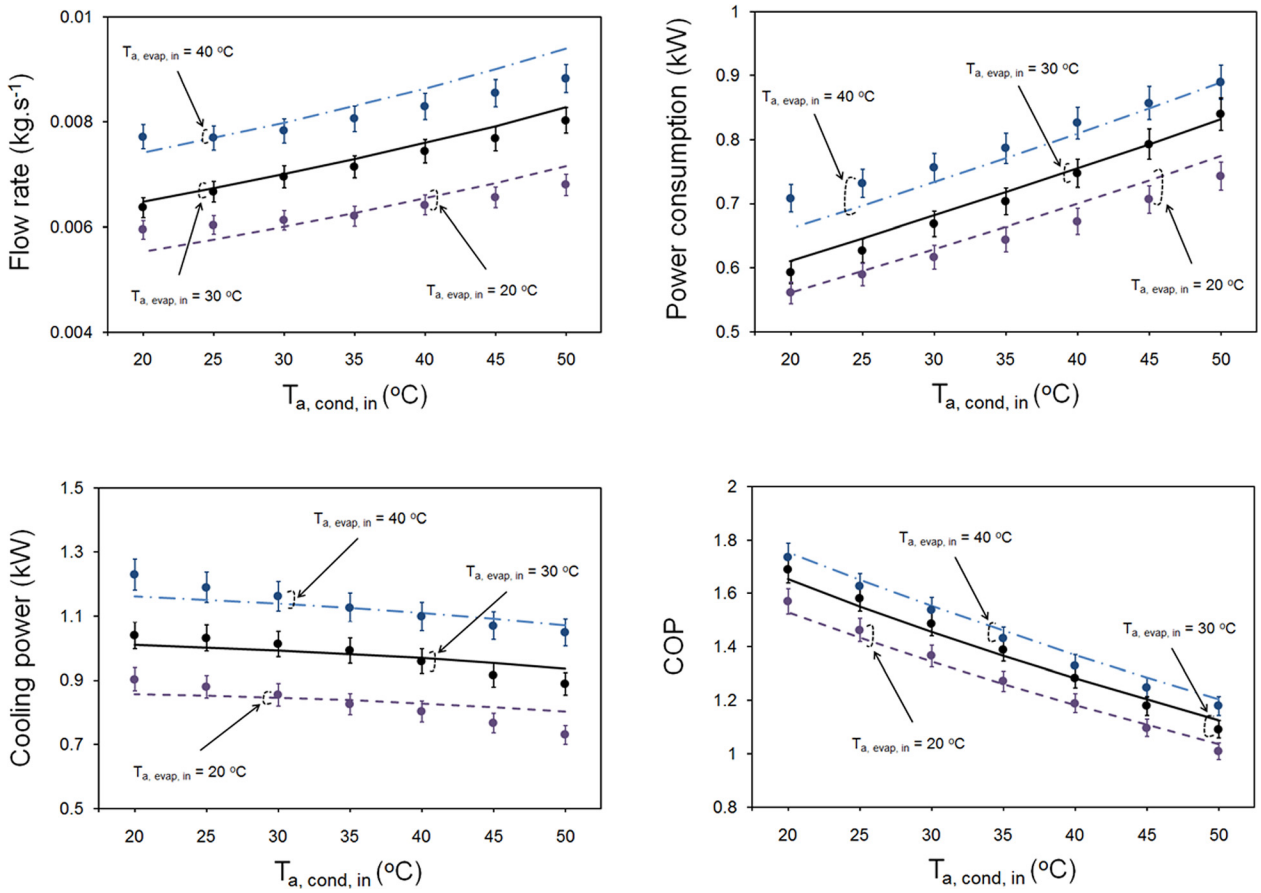

Fig. 6 Verification of the model results (lines) with experimental data (symbols)

decreases. Consequently, for any constant $T_{a,\text{evap,in}}$, the power consumption increment and the cooling power decrement by increasing $T_{a,\text{cond,in}}$ lead to a COP reduction. Based on these verified results, the performance of system significantly drops in warmer ambient conditions (higher $T_{a,\text{cond,in}}$); however, it slightly increases by increasing the temperature of conditioned space (higher $T_{a,\text{evap,in}}$).

4.3 Optimum Performance by Evaporator and Condenser Fans' Speed Variation—Modeling Results. As described in Sec. 3, the employed BPVAC system in this study is equipped with a constant speed compressor and two variable speed fans. Therefore, the adjustment of evaporator and condenser fans' speed, which affects the power consumption as well as the cooling power, can be an area of performance optimization for the system. To investigate the effects of fans' speed on the system performance, in this section, a wide range of the condenser air flow rate $\dot{m}_{a,\text{cond}}$ and the evaporator air flow rate $\dot{m}_{a,\text{evap}}$ is modeled, and the results are presented. For all the results of this section, the refrigerant charge is assumed to be kept at the obtained optimum value of 0.75 kg (Sec. 4.1) to achieve the highest performance. It should be mentioned that based on the performed experiments, the optimum charge does not change sensibly by operational conditions.

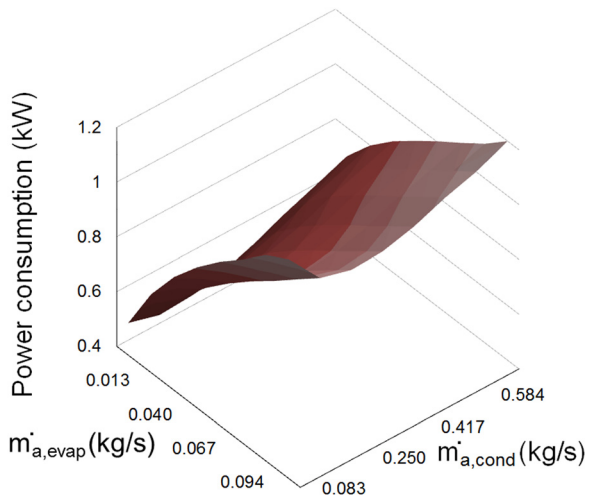

Fig. 7 Total power consumption versus condenser and evaporator air flow rates ($\dot{m}_{a,\text{cond}}$, $\dot{m}_{a,\text{evap}}$)

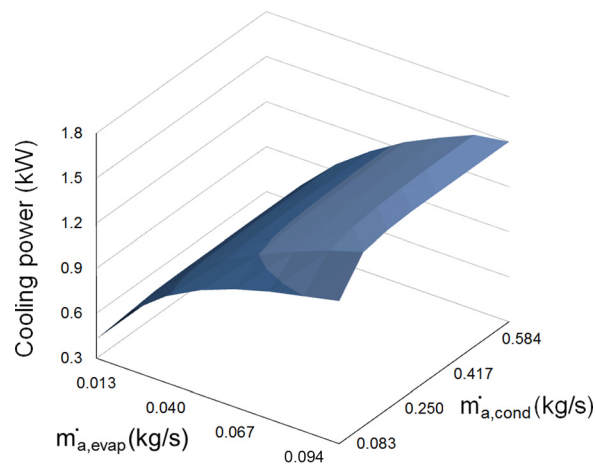

Fig. 8 Cooling power versus condenser and evaporator air flow rates ($\dot{m}_{a,\text{cond}}$, $\dot{m}_{a,\text{evap}}$)

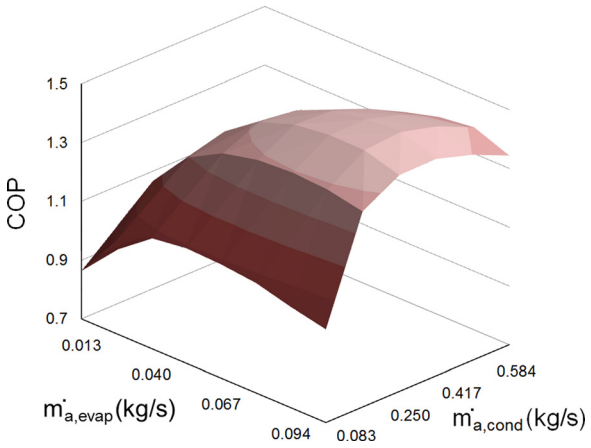

Fig. 9 COP versus condenser and evaporator air flow rates ($\dot{m}_{a,cond}$, $\dot{m}_{a,evap}$)

As such, changing the fans' speed that leads to variation in operational conditions does not affect the found optimum charge of refrigerant for the system.

A wide range of applicable evaporator and condenser fans' speed are simulated in this section. For this purpose, the air flow rate through condenser ($\dot{m}_{a,cond}$) and evaporator ($\dot{m}_{a,evap}$) that represents the condenser and evaporator fans' speed is varied in the model. However, the ranges of variation for the rotational speed of condenser and evaporator fans are restricted. A small speed of the evaporator fan leads to frost formation on the evaporator coil. Furthermore, a large speed of the evaporator fan may cause noise and discomfort for the people in the conditioned space. For the condenser fan, a small rotational speed may bring to insufficient heat rejection from the condenser coil that reduces the compressor lifetime. In addition, a large speed for the condenser fan brings to a noisy and inefficient operation of the system.

In Figs. 7–9, the behavior of power consumption, cooling power, and COP of the system for a wide range of $\dot{m}_{a,cond}$ and $\dot{m}_{a,evap}$ is plotted. For all the presented results, the evaporator and condenser air inlet temperatures ($T_{a,evap,in}$, $T_{a,cond,in}$) are kept equal to 26.7 and 35 °C, respectively, based on ANSI/AHRI 210/240-2008. The simulations are also performed for other operational conditions, and similar trends are obtained. Based on the obtained results, the following can be concluded:

- The condenser air flow rate $\dot{m}_{a,cond}$ (or condenser fan speed) affects the condensing temperature that has direct relationship with condensing pressure. By increasing $\dot{m}_{a,cond}$, the condensing temperature decreases which results in lower condensing pressure that reduces the compressor power consumption. However, the power consumption of condenser fan increases by increasing $\dot{m}_{a,cond}$. Eventually, by increasing $\dot{m}_{a,cond}$, the total power consumption first decreases to a point of minimum power due to predominance of compressor power reduction, and then starts increasing due to predominance of condenser fan power increment (see Fig. 7).
- The evaporator air flow rate $\dot{m}_{a,evap}$ (or evaporator fan speed) is directly proportional to the cooling power of system. Increasing $\dot{m}_{a,evap}$ for any $\dot{m}_{a,cond}$ brings to an increment of the cooling power due to increment of the heat transfer rate through the evaporator. Also, the condenser air flow rate $\dot{m}_{a,cond}$ is an effective parameter on the cooling power because of changing the condensing pressure that affects the refrigerant mass flow rate and the cycle pressure ratio. Totally, the cooling power increases by increasing either $\dot{m}_{a,cond}$ or $\dot{m}_{a,evap}$; however, the rate of increment at smaller $\dot{m}_{a,cond}$ or $\dot{m}_{a,evap}$ is more remarkable (see Fig. 8).
- For any constant $\dot{m}_{a,evap}$, by increasing $\dot{m}_{a,cond}$, the COP of system first increases to a point of maximum value because of the cooling power increment and the power consumption decrement, and then it starts to decrease that leaves a point of maximum COP for the system (see Fig. 9).
- The magnitude of the maximum COP of system increases by increasing $\dot{m}_{a,evap}$ until it reaches a point beyond which the maximum COP starts to decrease. That point returns the optimum simultaneous setting of both fans to achieve the highest COP of the system, see Fig. 9. This figure shows that although the rate of maximum COP variations is significant at smaller $\dot{m}_{a,evap}$, it becomes nearly negligible at larger $\dot{m}_{a,evap}$.
- The maximum obtained COP of the system under ANSI/AHRI 210/240-2008 condition is 1.49, which is achievable by setting the evaporator and condenser fans' speeds to blow 0.085 and 0.333 kg/s flow rates, respectively. Thus, if the fans are adjusted to blow the abovementioned flow rates, the COP can be enhanced from 1.35, previously found in Sec. 4.1 for the nominal speeds of the fans, to 1.49. This adjustment brings to 10.5% performance improvement of the VAC system under the same operational condition.

The simulations are also performed for other air-side temperatures than the ANSI/AHRI 210/240-2008 specifications that show similar trends for power consumption, cooling power, and COP of the system. Therefore, it is concluded that for any desired conditioned room temperature (cabin temperature of vehicle in BPVAC system) and any ambient temperature, optimum evaporator and condenser fans' speed (corresponding to optimum $\dot{m}_{a,evap}$, $\dot{m}_{a,cond}$) can be obtained to achieve the highest COP of the system. Based on this finding, the performance of existing BPVAC system (and any other VAC system equipped with variable speed fans) can be significantly improved to achieve a high level of energy conservation by designing a controller that first simulates the VAC system and finds its optimum evaporator and condenser fans' speeds (those contribute to the highest COP) and then commands the fans accordingly.

5 Conclusions

This paper presented a mathematical and experimental investigation into the performance of a battery-powered vehicle air conditioning (BPVAC) system as a promising alternative for green and sustainable energy transportation. A mathematical model was developed, and a test-bed was built using a typical BPVAC system. Various temperature, pressure, electric power, and flow rate measuring devices were utilized in the test-bed to collect real-time data for the mathematical model verification and experimental study. Utilizing the experimental setup and the verified model, a comprehensive study on the thermal and performance characteristics of the BPVAC system for a wide range of effective parameters, including refrigerant charge as well as condenser and evaporator air flow rates, was carried out. The followings were concluded from the study:

- Increasing the refrigerant charge from a relatively low quantity increases the cycle pressure ratio, power consumption, cooling power, and COP. However, after a specific range of charge, the cooling power and COP drop and the pressure ratio variation becomes smaller, while the power consumption continuously increases. Therefore, there is an optimum amount of refrigerant charge that results in maximum COP for the system (0.75 kg of HFC-134a for the studied system that results in COP = 1.35).
- The COP decreases by increasing the condenser air inlet temperature ($T_{a,cond,in}$) for any constant evaporator air inlet temperature ($T_{a,evap,in}$) due to the cooling power reduction and power consumption increment.
- Increasing the evaporator air flow rate ($\dot{m}_{a,evap}$), which represents the evaporator fan speed increment, for any constant condenser air flow rate ($\dot{m}_{a,cond}$) increases the cooling power

and total power consumption of the system. The rate of such increments is more significant at smaller $\dot{m}_{a,\text{evap}}$ values.

- Increasing $\dot{m}_{a,\text{cond}}$ (equivalent to increasing the speed of condenser fan) for any constant $\dot{m}_{a,\text{evap}}$ slightly increases the cooling power of the system. However, due to decrease of the power consumption by the compressor and increase of the power consumption by the condenser fan, the total power consumption of the system first decreases (at lower $\dot{m}_{a,\text{cond}}$) and then increases (at higher $\dot{m}_{a,\text{cond}}$). Eventually, the COP first increases and then decreases that leaves a point of maximum COP for the system. The results showed that there is a potential of 10.5% performance improvement for the system only by changing the fans' speed under a same condition of ANSI/AHRI 210/240-2008.
- Based on the obtained COP behavior, the performance of existing BPVAC systems can be remarkably optimized by frequent checking of the refrigerant charge (to be kept at optimum amount) and ambient-based controlling of the fans' speed. This achievement is expandable to all VAC systems equipped with variable speed fans. As such, a significant amount of energy can be conserved globally by utilizing the obtained concept to develop the intelligent fans' speed controllers for the VAC systems.

Acknowledgment

This work was supported by the Automotive Partnership Canada (APC), Grant No. APCPJ 401826-10. The authors would like to thank kind support from the Cool-It Group, #100–663 Sumas Way, Abbotsford, BC, Canada.

Nomenclature

C = thermal capacity ($\text{W} \cdot ^\circ\text{C}^{-1}$)
c_0 to c_3 = fan power consumption constants
C^* = thermal capacity ratio ($C_{\min}.C_{\max}^{-1}$)
g_1 to g_{20} = model equations
h = enthalpy ($\text{kJ}\,(\text{kg}\cdot^\circ\text{C})^{-1}$)
$\dot{m}$ = mass flow rate ($\text{kg}\,\text{s}^{-1}$)
N = compressor rotational speed (rps)
NTU = number of transfer units
Nu = Nusselt number
P = pressure (kPa)
Pr = Prandtl number
$\dot{Q}$ = heat transfer rate (W)
Re = Reynolds number
T = temperature ($^\circ$C)
UA = overall heat transfer coefficient ($\text{W} \cdot ^\circ\text{C}^{-1}$)
V = compressor displacement ($\text{m}^3\,\text{r}^{-1}$)
W = power consumption (kW)
x_1 to x_{20} = model variables
γ = vapor quality

Subscripts/Superscripts

a = air
c = condensing
comp = compressor
cond = condenser
cr = critical
e = evaporating
E = electrical
evap = evaporator
f = fan
g = gas
in = inlet
l = liquid
M = mechanical
max = maximum
min = minimum
n = iteration step number
nom = nominal
out = outlet
ref = refrigerant
TEV = thermostatic expansion valve
v = volumetric
1 − ph = one-phase flow
2 − ph = two-phase flow

Greek Symbols

ε = heat exchanger effectiveness
η = efficiency
ρ = density ($\text{kg}\,\text{m}^{-3}$)

References

[1] Gaines, L., Rask, E., and Keller, G., 2012, "Which is Greener: Idle, or Stop and Restart? Comparing Fuel Use and Emissions for Short Passenger Car Stops," TRB 2013 Annual Meeting.
[2] Gaines, L., 2012, "Idling Reduction for Medium-Duty Fleets," Green Fleets Conference, Schaumberg, IL, Oct. 2–3.
[3] Stodolsky, F., Gaines, L., and Vyas, A., 2000, "Analysis of Technology Options to Reduce the Fuel Consumption of Idling Trucks," Center for Transportation Research, Argonne National Laboratory, U.S. Department of Energy, Report No. ANL/ESD-43.
[4] MacDonald, C., Douglas, R., Tamayol, A., and Bahrami, M., 2012, "A Feasibility Study of Auxiliary HVAC Systems for Reducing Idling Time of Long Haul Trucks," ASME Paper No. HT2012-58353.
[5] Afram, A., and Janabi-Sharifi, F., 2014, "Review of Modeling Methods for HVAC Systems," Appl. Therm. Eng., **67**(1–2), pp. 507–519.
[6] Anand, S., Gupta, A., and Tyagi, S. K., 2013, "Simulation Studies of Refrigeration Cycles: A Review," Renewable Sustainable Energy Rev., **17**, pp. 260–277.
[7] Ding, G., 2007, "Recent Developments in Simulation Techniques for Vapour-Compression Refrigeration Systems," Int. J. Refrig., **30**(7), pp. 1119–1133.
[8] Hermes, C. J. L., Melo, C., Knabben, F. T., and Gonçalves, J. M., 2009, "Prediction of the Energy Consumption of Household Refrigerators and Freezers Via Steady-State Simulation," Appl. Energy, **86**(7–8), pp. 1311–1319.
[9] Boeng, J., and Melo, C., 2014, "Mapping the Energy Consumption of Household Refrigerators by Varying the Refrigerant Charge and the Expansion Restriction," Int. J. Refrig., **41**, pp. 37–44.
[10] Lee, G. H., and Yoo, J. Y., 2000, "Performance Analysis and Simulation of Automobile Air Conditioning System," Int. J. Refrig., **23**(3), pp. 243–254.
[11] Cho, H., Lee, H., and Park, C., 2013, "Performance Characteristics of an Automobile Air Conditioning System With Internal Heat Exchanger Using Refrigerant R1234yf," Appl. Therm. Eng., **61**(2), pp. 563–569.
[12] Green, T., Izadi-Zamanabadi, R., Razavi-Far, R., and Niemann, H., 2014, "Plant-Wide Dynamic and Static Optimisation of Supermarket Refrigeration Systems," Int. J. Refrig., **38**, pp. 106–117.
[13] Al-Rashed, A. A. A. A., 2011, "Effect of Evaporator Temperature on Vapor Compression Refrigeration System," Alexandria Eng. J., **50**(4), pp. 283–290.
[14] Sahin, B., and Kodal, A., 2002, "Thermoeconomic Optimization of a Two Stage Combined Refrigeration System: A Finite-Time Approach," Int. J. Refrig., **25**(7), pp. 872–877.
[15] Joudi, K. A., Mohammed, A. S. K., and Aljanabi, M. K., 2003, "Experimental and Computer Performance Study of an Automotive Air Conditioning System With Alternative Refrigerants," Energy Convers. Manage., **44**(18), pp. 2959–2976.
[16] Han, X. H., Li, P., Xu, Y. J., Zhang, Y. J., Wang, Q., and Chen, G. M., 2013, "Cycle Performances of the Mixture HFC-161 + HFC-134a as the Substitution of HFC-134a in Automotive Air Conditioning Systems," Int. J. Refrig., **36**(3), pp. 913–920.
[17] Yoo, S. Y., and Lee, D. W., 2009, "Experimental Study on Performance of Automotive Air Conditioning System Using R-152a Refrigerant," Int. J. Automot. Technol., **10**(3), pp. 313–320.
[18] Brown, J. S., Yana-motta, S. F., and Domanski, P. A., 2002, "Comparitive Analysis of an Automotive Air Conditioning Systems Operating With CO_2 and R134a," Int. J. Refrig., **25**(1), pp. 19–32.
[19] Ratts, E. B., and Brown, J. S., 2000, "An Experimental Analysis of Cycling in an Automotive Air Conditioning System," Appl. Therm. Eng., **20**(11), pp. 1039–1058.
[20] Wang, S., Gu, J., Dickson, T., Dexter, J., and McGregor, I., 2005, "Vapor Quality and Performance of an Automotive Air Conditioning System," Exp. Therm. Fluid Sci., **30**(1), pp. 59–66.
[21] Macagnan, M. H., Copetti, J. B., Souza, R. B., Reichert, R. K., and Amaro, M., 2013, "Analysis of the Influence of Refrigerant Charge and Compressor Duty Cycle in an Automotive Air Conditioning System," 22nd International Congress of Mechanical Engineering (COBEM 2013), Ribeirao Preto, Brazil, Nov. 3–7, pp. 6151–6161.
[22] Alkan, A., and Hosoz, M., 2010, "Comparative Performance of an Automotive Air Conditioning System Using Fixed and Variable Capacity Compressors," Int. J. Refrig., **33**(3), pp. 487–495.
[23] Jabardo, J. M. S., Mamani, W. G., and Ianella, M. R., 2002, "Modeling and Experimental Evaluation of an automotive Air Conditioning System With a Variable Capacity Compressor," Int. J. Refrig., **25**(8), pp. 1157–1172.

[24] Tian, C., and Li, X., 2005, "Numerical Simulation on Performance Band of Automotive Air Conditioning System With a Variable Displacement Compressor," Energy Convers. Manage., **46**(17), pp. 2718–2738.
[25] Koury, R. N. N., Machado, L., and Ismail, K. A. R., 2001, "Numerical Simulation of a Variable Speed Refrigeration System," Int. J. Refrig., **24**(2), pp. 192–200.
[26] Borges, B. N., Hermes, C. J. L., Gonçalves, J. M., and Melo, C., 2011, "Transient Simulation of Household Refrigerators: A Semi-Empirical Quasi-Steady Approach," Appl. Energy, **88**(3), pp. 748–754.
[27] Shah, R. K., and Sekulic, D. P., 2003, *Fundamentals of Heat Exchanger Design*, Wiley, Hoboken, NJ.
[28] Liang, N., Shao, S., Tian, C., and Yan, Y., 2010, "Dynamic Simulation of Variable Capacity Refrigeration Systems Under Abnormal Conditions," Appl. Therm. Eng., **30**(10), pp. 1205–1214.
[29] Browne, M. W., and Bansal, P. K., 2002, "Transient Simulation of Vapour-Compression Packaged Liquid Chillers," Int. J. Refrig., **25**(5), pp. 597–610.
[30] Beatty, K., and Katz, D., 1948, "Condensation of Vapours on the Outside of Finned Tube," Chem. Eng. Prog., **44**(1), pp. 66–70.
[31] Zhao, L., Cai, W., Ding, X., and Chang, W., 2013, "Model-Based Optimization for Vapor Compression Refrigeration Cycle," Energy, **55**, pp. 392–402.
[32] Jolly, P. G., Tso, C. P., Wong, Y. W., and Ng, S. M., 2000, "Simulation and Measurement on the Full-Load Performance of a Refrigeration System in a Shipping Container," Int. J. Refrig., **23**(2), pp. 112–126.
[33] Abbasbandy, S., 2003, "Improving Newton–Raphson Method for Nonlinear Equations by Modified Adomian Decomposition Method," Appl. Math. Comput., **145**(2–3), pp. 887–893.
[34] Tassou, S. A., and Grace, I. N., 2005, "Fault Diagnosis and Refrigerant Leak Detection in Vapour Compression Refrigeration Systems," Int. J. Refrig., **28**(5), pp. 680–688.
[35] Grace, I. N., Datta, D., and Tassou, S. A., 2005, "Sensitivity of Refrigeration System Performance to Charge Levels and Parameters for On-Line Leak Detection," Appl. Therm. Eng., **25**(4), pp. 557–566.